Scripta Materialia 144 (2018) 36–39

Contents lists available at ScienceDirect

Scripta Materialia

journal homepage: www.elsevier.com/locate/scriptamat

Regular Article

Selective generation of Ag interstitial defects in Te-rich $Bi_2(Te,Se)_3$ using Ag nanoparticles causing significant improvement in thermoelectric performance

Cham Kim [a,*], Su Yeol Jung [a], David Humberto Lopez [b], Dong Hwan Kim [a], Hoyoung Kim [a]

[a] Daegu Gyeongbuk Institute of Science and Technology (DGIST), 333 Techno Jungang-daero, Daegu 42988, Republic of Korea
[b] Department of Chemical and Environmental Engineering, University of Arizona, 1133 E. James. E. Rogers Way, Tucson, AZ, 85721, USA

ARTICLE INFO

Article history:
Received 31 July 2017
Accepted 25 September 2017

Keywords:
Thermoelectric materials
Lattice defects
Interstitials
Point defects
Thermoelectric transport properties

ABSTRACT

We report significant enhancement in thermoelectric performance of n-type $Bi_2(Te,Se)_3$ prepared via conventional melting process. We deposited chemically synthesized Ag nanoparticles onto Te-rich $Bi_2(Te,Se)_3$ and sintered the resulting substance to obtain a bulk product. The Ag nanoparticles and excessive Te elements should be converted to interstitial and antisite defects in the product, respectively, which possibly interacted to vary thermoelectric transport properties of the product. We endeavored to balance the concentration of the defects to optimize the properties, and thus we strengthened phonon glass electron crystal characteristic of the product, resulting in the improvement in thermoelectric performance.

N-type $Bi_2(Te,Se)_3$ and p-type $(Bi,Sb)_2Te_3$ in bulk phase have been primarily used for commercial thermoelectric applications at low temperatures (below 200 °C). Because the n-type $Bi_2(Te,Se)_3$ has generally exhibited lower thermoelectric performance than the p-type counterpart, it is required for the former to enhance the performance. The comprehensive thermoelectric performance is evaluated via the dimensionless figure of merit ZT ($=\alpha^2\sigma T/\kappa$), where α is the Seebeck coefficient, σ is the electrical conductivity, T is the absolute temperature, and κ is the thermal conductivity [1–6]; thus, the enhancement in the thermoelectric performance has been accomplished by increasing the electrical properties and by reducing the thermal conductivity, indicative of phonon glass electron crystal (PGEC) characteristic [7–15]. We suggested the way to improve thermoelectric performance of commercially applicable $Bi_2(Te,Se)_3$, which was prepared via a conventional melting process, in the present study. Te-rich $Bi_2(Te,Se)_3$ was employed as a reference, which should have Te_{Bi} antisite defects causing high carrier concentration and electrical conductivity. Ag nanoparticles (Ag NPs) were subsequently added to the reference to induce Ag-related defects, and thus the carrier concentration could be adjusted, which led to optimized combination of electrical conductivity and Seebeck coefficient, that is enhanced power factor. The Ag-related defects should also act as point defects for phonon scattering, which were expected to reduce thermal conductivity. Consequently, we concurrently regulated the Te_{Bi} antisite defects and Ag-related defects in the Te-rich $Bi_2(Te,Se)_3$ to maximize the power factor and to minimize the thermal conductivity, namely the PGEC characteristic, thus affording significant enhancement in figure of merit.

Ag-added $Bi_2(Te,Se)_3$ powders were prepared by depositing Ag NPs, which were synthesized by reducing an Ag precursor, onto the compound. A conventional pulverization method was employed to obtain the $Bi_2(Te,Se)_3$ powder. The raw metal elements (Bi, Te, and Se granules, 99.99%, Vital Materials) were weighed to a composition of the compound and mixed in a quartz tube, which was then evacuated below 10^{-5} Torr and sealed. The tube was heated to 1000 °C in a rocking furnace for 24 h and was cooled to room temperature. A resulting ingot was crushed into the powder, which was transferred into 4 mM of an $NaBH_4$ aqueous solution with vigorous stirring. 2 mM of an $AgNO_3$ aqueous solution was then added dropwise, and thus $AgNO_3$ could be reduced by $NaBH_4$ to form Ag NPs, which should be instantly deposited onto the $Bi_2(Te,Se)_3$ compound. The $AgNO_3$ reduction using $NaBH_4$ for Ag NPs has been reported elsewhere [16]. The amount of Ag NPs was adjusted by adding different amount of $AgNO_3$, thus affording the compounds with the different fractions of Ag NPs ranging from 0.1 to 0.4 wt%. After these mixed solutions were aged overnight, they were filtered to recover solid substances. The resulting substances were rinsed using dry ethanol and deionized water and were dried at 40 °C under vacuum to gain the compound powders including different amount of Ag NPs. We tried to pack the resultant powders using a spark plasma sintering equipment (SPS; DR. Sinter, SPS-3, 20MK-IV). Approximately each 15 g of the powders was individually placed into cylindrical graphite molds (55 × 60 mm^2 (d × h)) with an inner hole of 20 mm in

* Corresponding author.
E-mail address: charming0207@dgist.ac.kr (C. Kim).

https://doi.org/10.1016/j.scriptamat.2017.09.040
1359-6462/

diameter for compaction at 500 °C for 3 min. under a pressure of 50 MPa in an Ar atmosphere, resulting in the production of cylindrical bulk specimens (20×30 mm^2 (d × h)). Considering the typical anisotropic nature of Bi_2Te_3-based rhombohedral crystals, we took only perpendicular faces to the pressing direction in the specimens for thermoelectric characterizations. Details for the characterizations were given in the Supplementary material 1.

The diffraction pattern of the $Bi_2(Te,Se)_3$ specimen without Ag NPs (Fig. 1a, Pristine) exactly corresponded to JCPDS card No. 50-0954, which is the typical rhombohedral crystalline structure of $Bi_2Te_{2.7}Se_{0.3}$. We found no diffraction peaks for any Ag-related secondary phases although we increased the fraction of Ag NPs. Considering that Ag presence in the specimen was confirmed by Energy Dispersive X-ray Spectroscopy (EDS) mapping (Supplementary material 2), the Ag NP fractions should be too low to be detected by the XRD analysis. According to the XPS spectra of Ag 3d (Fig. 1b), Ag-associated traces were detected for the Ag NP added specimens – the signals for Ag $3d_{5/2}$ (367.5 eV) and Ag $3d_{3/2}$ (373.4 eV) began to come up when the fraction was 0.3 wt% and they strengthened as more Ag NPs were added to the compound. As the fraction increased, the XRD peak was coherently shifted to lower diffraction angle (Fig. 1a inlet), associated with lattice expansion due to the increase in lattice parameters (Supplementary material 3). Based on these results, Ag was not simply mixed with the compound but it was expected to occupy some crystal sites in the compound. Te has somewhat higher electronegativity than Bi but the difference is known to be small enough to generate either Te_{Bi} or Bi_{Te} antisite defect in Bi_2Te_3-based materials (Eq. (1a) and Eq. (1b)) [17]. These defects should bring about vacancies such as V_{Te} or V_{Bi} (Eq. (1a) and Eq. (1b)). The defects and vacancies contribute to the generation of electrons and holes, and thus the material's carrier concentration can be adjusted. Because an electron is a major carrier for an n-type semiconductor, Te_{Bi} should be dominant for n-type Bi_2Te_3 [18]. Our $Bi_2(Te,Se)_3$ was considered to have Te_{Bi} rather than Bi_{Te} because it strongly exhibited n-type characteristics (Supplementary material 4). In addition, the $Bi_2(Te,Se)_3$ showed higher carrier concentration than $Bi_2Te_{2.7}Se_{0.3}$ due to its higher stoichiometric ratio for Te, which resulted in the decrease in both electrical resistivity and Seebeck coefficient (Supplementary material 4). This could be also indicative of the dominant generation of Te_{Bi} in the $Bi_2(Te,Se)_3$ (Eq. (1a)). Therefore, Ag atoms were expected rather to contribute to the reduction of V_{Te} concentration (Eq. (2a)) by occupying the interstitial sites at the van der Waals gaps between $Te^{(1)}$ layers (i.e., Ag_i, Supplementary material 5), resulting in the decrease in carrier concentration (Eq. (2a)), than to take up V_{Bi} (i.e., Ag_{Bi}) (Eq. (2b)).

$$Bi_{Bi} + Te_{Te} \rightarrow Te^{\bullet}_{Bi} + V^{\bullet\bullet}_{Te} + 3e^- \quad (1a)$$

$$Bi_{Bi} + Te_{Te} \rightarrow Bi'_{Te} + V'''_{Bi} + 4h^+ \quad (1b)$$

$$Ag + V^{\bullet\bullet}_{Te} + 2e^- \rightarrow Ag^{\bullet}_{i} + e^- \quad (2a)$$

$$Ag + V'''_{Bi} + 3h^+ \rightarrow Ag'''_{Bi} + 2h^+ \quad (2b)$$

Some research groups have tried to prepare Ag-doped Bi_2Te_3-based materials via melting process [19] or powder metallurgy [20,21]. They reported that Ag atoms should occupy either the interstitial sites or the V_{Bi} sites in Bi_2Te_3 depending on the doping concentration, resulting in interstitial defects (Ag_i) or antisite defects (Ag_{Bi}), respectively. While Ag_i caused the decrease in carrier concentration as explained above (Eq. (2a)), Ag_{Bi} serves the removal of a hole carrier causing the increase in carrier concentration (Eq. (2b)). These opposite natures of the defects should interfere with the adjustment of carrier concentration for optimizing the electrical properties of our $Bi_2(Te,Se)_3$. We attempted to separate the $Bi_2(Te,Se)_3$ preparation process from Ag addition procedure by depositing Ag NPs onto the compound via the chemical process. During the following SPS process, the Ag NPs should react with the compound, and thus Ag atoms seemed to mainly occupy the interstitial sites to form Ag_i. The lattice parameters for c-axis increased with the Ag addition while those for a-axis did not show considerable change (Supplementary material 3), indicative of Ag_i presence at the van der Waals gaps rather than Ag_{Bi} generation in the lattice structure, which should be detected as the Ag traces in the XPS spectra (Fig. 1b). When comparing the peaks for Te 3d of the pristine $Bi_2(Te,Se)_3$ to those of the compounds with Ag NPs, we observed consistent peak shifts to lower binding energy with the increase in Ag NP fraction (Fig. 1c). It is well known that binding energy of core electrons in an element decreases when it is combined with a less electronegative element [22]. As elucidated above, Ag atoms were expected to occupy the interstitial sites at the

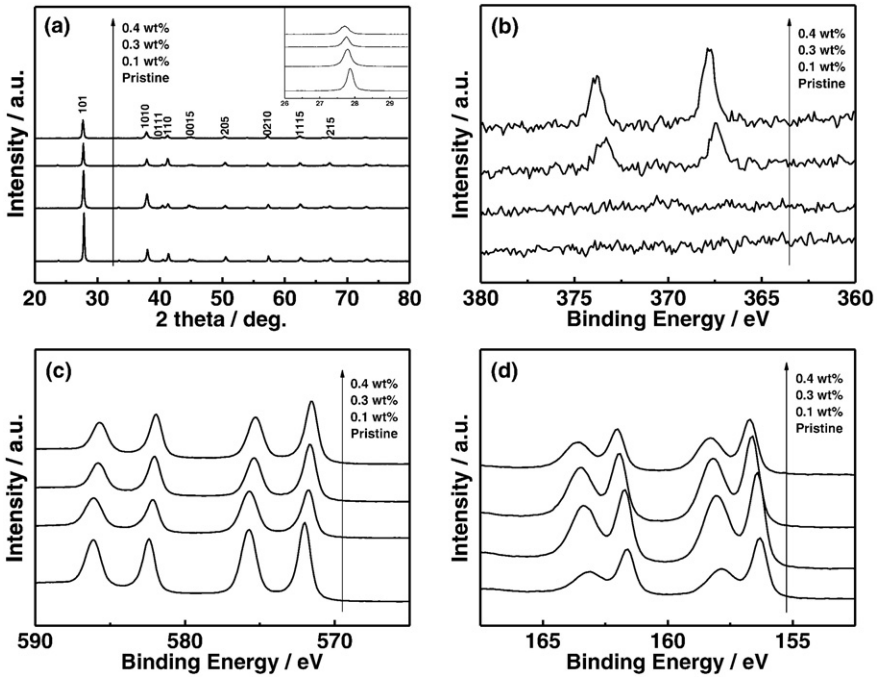

Fig. 1. Variation in XRD patterns (a) and XPS spectra for Ag 3d (b), Te 3d (c), and Bi 4f (d) of the $Bi_2(Te,Se)_3$ compound caused by Ag NP addition.